Published in final edited form as:
Epilepsy Res. 2015 January ; 0: 13–27. doi:10.1016/j.eplepsyres.2014.10.003.

Chronic stress shifts the GABA reversal potential in the hippocampus and increases seizure susceptibility

Georgina MacKenzie[1] and **Jamie Maguire**[1,*]

[1]Department of Neuroscience, Tufts University School of Medicine, Boston, MA, USA

Abstract

The most commonly reported precipitating factor for seizures is stress. However, the underlying mechanisms whereby stress triggers seizures are not yet fully understood. Here we demonstrate a potential mechanism underlying changes in neuronal excitability in the hippocampus following chronic stress, involving a shift in the reversal potential for GABA (E_{GABA}) associated with a dephosphorylation of the potassium chloride co-transporter, KCC2. Mice subjected to chronic restraint stress (30 mins/day for 14 consecutive days) exhibit an increase in serum corticosterone levels which is associated with increased susceptibility to seizures induced with kainic acid (20 mg/kg). Following chronic stress, but not acute stress, we observe a dephosphorylation of KCC2 residue S940, which regulates KCC2 cell surface expression and function, in the hippocampus. To determine the impact of alterations in KCC2 expression following chronic stress, we performed gramicidin perforated patch recordings to measure changes in E_{GABA} and neuronal excitability of principal hippocampal neurons. We observe a depolarizing shift in E_{GABA} in hippocampal CA1 pyramidal neurons after chronic stress. In addition, there is an increase in the intrinsic excitability of CA1 pyramidal neurons, evident by a shift in the input-output curve which could be reversed with the NKCC1 inhibitor, bumetanide. These data uncover a potential mechanism involving chronic stress-induced plasticity in chloride homeostasis which may contribute to stress-induced seizure susceptibility.

Keywords

KCC2; GABA; chronic stress; epilepsy

[*]Correspondence: Dr. Jamie Maguire, Department of Neuroscience, Tufts University School of Medicine, 136 Harrison Ave., SC205, Boston, MA, 02111, USA, Jamie.Maguire@tufts.edu.

AUTHOR CONTRIBUTIONS

G.M. carried out the vast majority of the experimental procedures, conducted the majority of the data analysis and interpretation of the data as well as wrote the first draft of the manuscript.

J.M. oversaw the design of this study, conducted some of the experiments, participated in the analysis and interpretation of the data, and writing of the manuscript.

Disclosures

No conflicts of interest, financial or otherwise, are declared by the authors.

Introduction

The hypothalamic-pituitary-adrenal (HPA) axis is activated in response to a stressful experience, resulting in the elevation of serum glucocorticoids (corticosterone in rodents and cortisol in humans) (Ulrich-Lai and Herman, 2009). Prolonged exposure can lead to maladaptive changes to the limbic system and increased vulnerability to mood disorders, cognitive deficits and epilepsy (Drevets et al., 2008; Joels and Baram, 2009; Lai and Trimble, 1997; Maguire and Salpekar, 2013; McEwen, 2012; McEwen and Gianaros, 2011; Pittenger and Duman, 2008; Ulrich-Lai and Herman, 2009). Chronic stress induces changes in hippocampal network and neuronal excitability, such as altered synaptic plasticity, dendritic atrophy and a loss of neurogenesis (Conrad, 2008; Joels et al., 2007; Joels and Baram, 2009; McEwen and Gianaros, 2011; Pavlides et al., 2002), which may predispose the hippocampus to seizure activity or exacerbate the symptoms of existing temporal lobe epilepsy

Epilepsy patients commonly report that stress is the main precipitating factor for seizures (for review see (Maguire and Salpekar, 2013)). Interestingly, in rodent studies an acute stressor has been shown to have anticonvulsant properties, an effect attributed to the production of neuroactive steroids which are positive modulators of $GABA_A$ receptors ($GABA_A$Rs) (Joels and Baram, 2009; Reddy and Rogawski, 2002); whereas, prolonged corticosterone administration or chronic exposure to a stressor increases seizure severity (Castro et al., 2012; Chadda and Devaud, 2004; Jones et al., 2013; Matsumoto et al., 2003) (for review see (Maguire and Salpekar, 2013)). However, despite the robust anecdotal evidence linking chronic stress with an increase in seizure susceptibility, the underlying mechanisms remain unclear.

Numerous studies have reported changes in hippocampal GABAergic signaling in both acute (de Groote and Linthorst, 2007; Maguire and Mody, 2007) and chronic stress models (Holm et al., 2011; Hu et al., 2010; Serra et al., 2008), suggesting that $GABA_A$Rs play an important role in mediating both the short and long term effects of stress. In the adult brain, the inhibitory actions of GABA are established by the potassium chloride co-transporter KCC2 which, by extrusion of chloride from the cell, maintains the $GABA_A$ reversal potential (E_{GABA}) below the resting membrane potential (RMP) (Payne et al., 1996; Payne et al., 2003). However, in the absence of KCC2 (for example in the immature brain and specific adult neuronal populations (Ben-Ari, 2002; Haam et al., 2012; Michelson and Wong, 1991; Sarkar et al., 2011; Song et al., 2011)), E_{GABA} is equal to or greater than the RMP, leading to shunting inhibition or membrane depolarization, respectively. The function of KCC2 is dependent on its cell surface expression and transport efficiency, which is tightly regulated by changes in phosphorylation states (Kahle et al., 2010; Kahle et al., 2013; Lee et al., 2007; Lee et al., 2010; Rinehart et al., 2011; Rivera et al., 2002; Rivera et al., 2004), allowing for rapid and readily reversible changes in the level of chloride extrusion. Alterations in KCC2 expression and function, where a loss or reduction in GABAergic inhibitory drive leads to increased neuronal excitability have been well characterized in pathophysiological states (Barmashenko et al., 2011; Ben-Ari et al., 2012; Bonislawski et al., 2007; Boulenguez et al., 2010; Papp et al., 2008; Pathak et al., 2007; Price et al., 2009). However, it is becoming increasingly clear that modifying chloride homeostasis is a normal

physiological regulatory response. Recently it has been shown that an acute restraint stress and early life stress leads to the downregulation of KCC2 and a shift in E_{GABA} in the parvocellular neurons of the paraventricular nucleus (PVN) (Gunn et al., 2013; Hewitt et al., 2009; Inoue and Bains, 2014; Sarkar et al., 2011) due to the dephosphorylation of serine residue 940 (S940) (Sarkar et al., 2011). These changes led to the collapse of the chloride gradient in CRH neurons, excitatory actions of GABA, and activation of the HPA axis.

Here we show for the first time that changes in chloride homeostasis also occur in the hippocampus after chronic but not acute stress. We observe a dephosphorylation of KCC2 residue S940 in the hippocampus after chronic stress and a loss of surface expression which coincides with a depolarizing shift in E_{GABA} and increased intrinsic excitability of CA1 pyramidal neurons. These changes are associated with an increase in susceptibility to kainic acid-induced seizures which could be rescued by blocking chloride influx through the sodium potassium chloride co-transporter (NKCC1) with bumetanide. These findings reveal one of the mechanisms contributing to increased neuronal excitability in the hippocampus following chronic stress which may contribute to stress-associated seizure susceptibility.

Materials and Methods

Animal handling

Adult male C57BL/6J mice were obtained from Jackson Lab and housed at the Tufts University School of Medicine, Division of Laboratory Animal Medicine. All mice were handled according to protocols approved by the Institutional Animal Care and Use Committee (IACUC). Mice were grouped housed (with a maximum of 5 mice/cage) with a 12 hour normal light/dark cycle (lights on at 7 a.m.) and *ad libitum* access to food and water. All experiments were performed during the light cycle. Modified clear polypropylene Falcon tubes (50 ml, 30×115 mm) with air holes drilled to allow for ample ventilation were used for restraint stress. Animals could rotate from a prone to supine position but the restraint tubes were small enough to prevent head to toe turning. The stressed group was subjected to a 30 minute restraint stress either once (acute stress group) or daily for 14 consecutive days (chronic stress group). Immediately following the final restraint stress mice were subjected to electroencephalogram (EEG) recording or anesthetized with isoflurane and sacrificed by decapitation where trunk blood was taken for corticosterone measurements (see below). All mice were 8–10 weeks old at the time of testing. Every attempt was made to minimize stress for the control group, which was minimally handled and allowed to acclimate to new surroundings in their home cage for at least 1 hour prior to testing.

Western Blotting

Western blotting was performed as previously described (Maguire et al., 2009; Maguire and Mody, 2007; Maguire et al., 2005; Sarkar et al., 2011). After isoflurane anesthesia, mice were euthanized by decapitation and the hippocampi were rapidly removed and sonicated in ice cold homogenization buffer containing (in mM): 10 $NaPO_4$, 10 sodium pyrophosphate, 100 NaCl, 25 NaF, 2% Triton X-100, 0.5% deoxycholate, 1 sodium vanadate, 5 EDTA, 5 EGTA, pH 7.4 and protease inhibitors (Complete Mini, Roche, and 1 mM fresh PMSF). The

lysate was incubated on ice for 30 minutes before centrifuging at 14,000 rpm for 10 minutes. The supernatant was collected and protein concentrations were determined using the DC protein assay kit (Biorad) as per the manufacturer's instructions. Total protein (50 μg) was loaded onto 10% SDS polyacrylamide gels, separated by gel electrophoresis and transferred to an Immobilin-P membrane (Millipore). The membrane was blocked in 10% non-fat milk and probed with either rabbit anti-KCC2 (1:1000, Millipore), rabbit anti-S940 (1:1000, a generous gift from Dr. Stephen Moss, Tufts University School of Medicine, Boston, MA, USA) or mouse anti-β-tubulin (1:10,000, Sigma). The membrane was then probed with peroxidase-labeled anti-rabbit or anti-mouse IgG (1:2000, GE Healthcare) and visualized using enhanced chemiluminescence (GE Healthcare). NIH ImageJ software was used for optical density measurements.

Biotinylation experiments were performed as described previously (Sarkar et al., 2011). Briefly, hippocampal slices were incubated in 1 mg/ml NHS-biotin (Pierce) in normal artificial CSF (aCSF, in mM): 126 NaCl, 26 $NaHCO_3$, 1.25 NaH_2PO_4, 2.5 KCl, 2 $CaCl_2$, 2 $MgCl_2$, 10 dextrose, 1 L-glutamine and 1.5 sodium pyruvate (300–310 mOsm/LH_20) for 30 min on ice. After thoroughly washing the slices with ice-cold aCSF the total protein was isolated and quantified as described above. 100 μg of total protein was then incubated in 1ml of PBS with 50 μl of streptavidin magnetic beads (Pierce) overnight at 4°C. The solution was centrifuged and the pellet washed and resuspended in 50 μl of loading buffer. Following elution, the magnetic beads were removed by centrifugation and 10μl of the protein/loading buffer solution was subjected to SDS-PAGE and probed for S940 and KCC2 as described above.

Corticosterone measurements

The serum was isolated from whole trunk blood by high speed centrifugation in serum collection tubes (Terumo, MD, USA) (14,000 rpm, 5 minutes). Corticosterone concentrations were measured in duplicate as described previously (Sarkar et al., 2011) using an enzyme immunoassay and compared to a standard curve of known corticosterone concentrations as per the manufacturer's instructions (Enzo Life Sciences). To minimize variability, all samples from each experiment were stored at −80°C before testing in parallel.

Electrophysiological recordings

Adult (8–10 week old) male mice were anesthetized with isoflurane, decapitated and the brain rapidly removed. The brain was immersed in ice cold aCSF supplemented with 3 mM kynurenic acid during the slicing procedure. Coronal sections (400 μm) were generated using a Leica vibratome and incubated at 33°C in a holding chamber containing normal aCSF for at least one hour prior to transferring to the recording chamber. The recording chamber was maintained at 33°C (in line heater, Warner Instruments) and perfused with aCSF at a rate of ≥ 4 ml/minute throughout the experiment. All solutions were continuously bubbled with 95% O_2 and 5% CO_2. GABA (5 μM), kynurenic acid (3 mM), SR95531 (Gabazine, ≥200 μM) and Bumetamide 10 μM were added to the extracellular solution where indicated. A 200B Axopatch amplifier (Molecular Devices), PowerLab Hardware and LabChart 7 data acquisition software (AD Instruments) were used for all recordings.

Input-output curves were generated from visually identified CA1 pyramidal neurons as previously described (Lee and Maguire, 2013). Neurons were injected with 500 ms square wave current injections increasing in 20 pA increments from 20–300 pA. Other than the square wave current injections, no additional current was applied during current clamp recordings. Gramicidin perforated patch recordings were used to maintain the native chloride ion gradients, whereas whole cell recordings (internal chloride concentration of 14 mM) were performed for comparison. A subset of whole cell recordings were performed in the same neurons as those used for perforated patch by moving to the whole cell configuration at the end of the perforated patch experiment. Borosilicate glass micropipettes (World Precision Instruments) with DC resistance of 5–8 MΩ were backfilled with internal solution containing (in mM): 130 K-gluconate, 10 KCl, 4 NaCl, 10 HEPES, 0.1 EGTA, 2 Mg-ATP, 0.3 Na-GTP (pH = 7.25, 280–290 mOsm/LH_2O) with 50 μg/ml gramicidin (ABCD, Sigma). The internal solution was gently vortex prior to experimentation. Upon generating a high resistance (> 1GΩ) seal, perforation was determined by the gradual increase in capacitive transients in response to a −5mV voltage step and the decrease in membrane resistance, which dropped below 200 MΩ within approximately 20 minutes following patch formation as described previously (O'Toole et al., 2013; Sarkar et al., 2011)) and $V_{pipette}$ reached a value close to the RMP similar to previous studies (Zhu et al., 2008). No significant difference in series resistance was observed between experimental groups. Series resistance and capacitive transients were periodically monitored throughout the experiment and data were immediately rejected if the resistance suddenly dropped and/or the membrane potential suddenly changed, indicating rupture of the patch (Yu et al., 2013). Each individual input-output curve was fit with a Boltzmann function: $f(W) = MAX/(1 + \exp((I_{50}\text{-}I)/k))$, where I is current injected, MAX is the maximum response, k is a slope factor, and I_{50} is the current injection amplitude that elicits 50% of MAX. To estimate the current required to reach action potential threshold (iAP), a linear regression was fit to the first 4 nonidentical data points (Figure 3d). APs generated in the whole cell configuration were further analyzed using phase plane plots (Bean, 2007) where the first derivative of the voltage is plotted against the voltage.

E_{GABA} was determined in the voltage clamp configuration using the perforated patch technique as described above. The internal solution contained (in mM): 140 KCl, 4 NaCl, 10 HEPES, 0.1 EGTA, 2 Mg-ATP, 0.3 Na-GTP, 2 QX314-Br (pH = 7.25, 280–290 mOsm) with 50 μg/ml gramicidin (ABCD, Sigma). The use of a high intracellular chloride concentration controlled for rupturing of the patch, which corresponded to the sudden increase in capacitive transient, membrane resistance and inwardly directed IPSCs. Data were immediately discarded when this occurred. 3 mM kynurenic acid was added to the aCSF to block AMPA and NMDA receptors. The RMP was determined in the I=0 recording configuration and measured both before and after application of 5 μM GABA to the external solution. No significant difference in RMP was observed in the presence or absence of external 5 μM GABA (data not shown). Recordings from CA1 pyramidal neurons were rejected if their RMP was greater than −50 mV or less than −85 mV. The current generated in response to 5 mV voltage steps (2 s duration) from −90 mV to −40 mV was used to plot the current-voltage (I–V) relationship (Song et al., 2011). The addition of 5μM GABA enables us to compare the relative shifts in E_{GABA} between experimental groups, but likely

does not reflect the absolute E_{GABA} values under physiological conditions. The difference in the I–V relationship in the presence or absence of SR95531 (≥400 μM applied directly to the bath) was used to extract the $GABA_A$ mediated current and the data fit with a 2nd order polynomial equation to determine E_{GABA} (Song et al. 2011). E_{GABA} values were excluded if the $GABA_A$ mediated I–V relationship failed to cross the x-axis between −90 and −40 mV. Shunting inhibition was defined as E_{GABA} values ± 1 mV from the resting potential.

Phasic and tonic GABAergic responses were recorded in CA1 pyramidal neurons voltage clamped at −60 mV in the whole cell configuration. The bath solution contained 3 mM kynurenic acid to block the glutamatergic synaptic responses and the internal solution contained (in mM) 140 CsCl, 1 $MgCl_2$, 10 HEPES, 4 NaCl, 0.1 EGTA, 2 Mg-ATP, 0.3 Na-GTP (pH = 7.25, 280–290 mOsm/LH_2O). Cells were subjected to a −10 mV voltage step to determine the input conductance. To reduce cellular variability input conductances were normalized to the cell capacitance and expressed as nS/pF.

Synaptic events were analyzed using winEDR (version 3.3.1) and winWCP software (version 4.5.8, kindly provided by John Dempster, University of Strathclyde, UK). Spontaneous IPSCs were detected using amplitude threshold crossing. Averaged IPSCs were constructed from events which exhibited a monotonic rise and an uninterrupted decay phase which were aligned on their initial rising phases. Events were selected over a 30 s epoch (a minimum of 50 events). The baseline current was determined using a 5 ms epoch immediately prior to the detected event with the peak current calculated relative to this value. The decay time constants were calculated as the integral of the averaged IPSCs divided by the peak current. To measure the tonic GABAergic conductance, the holding current during a 60 second epoch was measured before and after the addition of SR95531. Data were plotted as all points histograms and fitted with a single Gaussian function with the difference in the mean holding current before and after the addition of SR95531 (≥200μM) corresponding to the tonic conductance.

Electroencephalogram (EEG)

To measure seizure susceptibility, 6-week-old male mice were anesthetized with 100 mg/kg ketamine and 10 mg/kg xylazine and implanted with a headmount consisting of 2 differential cortical EEG and 1 differential EMG electrodes (Pinnacle Technology Inc., part #8201). Two leads were placed anterior to Bregma and two were place posterior to Bregma, with one anterior and posterior lead being placed in each hemisphere. After allowing a week for recovery, one cohort was subjected to the 14 day restraint stress paradigm whereas the control group was minimally handled. On the day of the final bout of restraint stress, a separate cohort of mice were subjected to a single episode of restraint stress (acute stress). The mice were then tethered to the Pinnacle Technology Inc. turnkey system (part #8200) with a 100x gain preamplifier high pass filtered at 1.0 Hz (part #8202-SE) and monitored using the PowerLab system and LabChart Pro software (AD Instruments). After a baseline recording period of 30 minutes, the animals were administered a single 10 mg/kg dose of kainic acid (i.p.) and the EEG recording continued for a 2 hour period. The bumetanide group were administered a single 0.2 mg/kg dose of bumetanide (i.p) following the final restraint and 30 minutes prior to kainic acid administration. The average duration and total

time exhibiting epileptiform activity were analyzed as described previously (Maguire and Mody, 2007; Maguire et al., 2005; O'Toole et al., 2013). Epileptiform activity included ictal events, which were defined as the sudden onset of high amplitude activity, at least 2.5 times the standard deviation of the baseline, lasting longer than 5 s in duration with consistent changes in the Power of the fast Fourier transform (FFT), and abnormal periods of EEG activity which cannot be defined as a seizure, including periods of low frequency, rhythmic electrographic spiking lasting longer than 30 s without a behavioral seizure component.

Statistical analyses

Statistical significance between two experimental groups (no-stress control and stress groups) was determined using an unpaired Student's t-test. A one-way ANOVA was used to compare between multiple experimental groups (control, acute and chronic stress or control, chronic stress and chronic stress with bumetanide) and significant interactions were explored using either Tukey or Dunnett's post hoc tests, as appropriate. A Chi Square test with contingency tables was used to compare neurons with depolarizing EGABA to those with shunting/hyperpolarizing E_{GABA} responses. All statistical calculations were performed using Graphpad Prism 6. Data in the text are presented as ± the Standard Error of the Mean (SEM).

Results

KCC2 is dephosphorylated in the hippocampus after chronic but not acute stress leading to a loss of surface expression

Our previous data demonstrated the dephosphorylation of KCC2 residue S940 and a downregulation of the transporter in the PVN following an acute restraint stress (a single 30 minute restraint), resulting in the switch from hyperpolarizing to depolarizing actions of GABA (Sarkar et al., 2011). Similar to the changes observed in the hypothalamus, we hypothesized that stress may also evoke a downregulation of KCC2 in the hippocampus, which is a region particularly vulnerable to the effects of stress (Joels et al., 2007), resulting in increased neuronal excitability and a greater vulnerability to seizures.

To validate that our stress paradigm induces a physiological response to stress, adult male C57Bl/6J mice were subjected to either an acute restraint stress (a single 30 minute restraint) or a chronic restraint stress paradigm (30 minutes of restraint stress daily for 14 consecutive days) and corticosterone levels were compared to minimally-handled controls. No significant difference in corticosterone levels were observed between the minimally handled controls used for the acute stress group (19.36 ± 2.58 ng/ml, n = 49) or the chronic stress group (14.25 ± 1.72 ng/ml, n = 78; $p > .05$ Student's unpaired t-test) therefore these values were pooled (17.45 ± 1.72 ng/ml, n = 103). As described previously (Hewitt et al., 2009; Sarkar et al., 2011), an acute 30 minute restraint stress was sufficient to generate a significant increase in serum corticosterone (246.85 ± 24.80 ng/ml, n = 34). Similarly, a significant increase in serum corticosterone levels was also observed in mice subjected to chronic restraint stress (281.46 ± 33.43 ng/ml; n = 76) ($p < 0.001$ using a one-way ANOVA ($F(2,210) = 50.94$) with a Tukey post hoc test).

To determine whether there is a loss of KCC2 phosphorylation at residue S940 in the hippocampus following stress, western blot analysis was carried out on the total protein isolated from the hippocampi of mice subjected to acute or chronic stress and minimally-handled controls. No difference in total KCC2 or the phosphorylation of KCC2 residue S940 was observed in the hippocampus after acute stress (S940 = 33.34 ± 4.48; total KCC2 = 53.67 ± 5.91 OD units for 50 μg protein; n =12) compared to minimally-handled controls (S940 = 30.06 ± 2.71; KCC2 = 51.72 ± 5.44 OD units/50 μg protein; n =12) (Figure 1a and 1b). Interestingly, although there was not a significant change in total KCC2 levels (control= 57.40 ± 5.15; chronic stress = 47.77 ± 4.74 OD units/50 μg protein), there was a significant reduction in the phosphorylation of KCC2 residue S940 after chronic stress (19.42 ± 2.11 OD units for 50 μg protein; n= 14) compared to control (28.26 ± 2.46 OD units/50 μg protein; n =13) (p = .011 using a Student's unpaired t-test) (Figure 1a and 1c), which may have a significant impact on transporter function and surface expression (Lee et al., 2007; Lee et al., 2011).

To determine whether the dephosphorylation of KCC2 at S940 reduced surface expression as described previously (Lee et al., 2011; Sarkar et al., 2011) biotinylation assays were performed following chronic stress and probed for KCC2 and S940 phosphorylation. These data demonstrated a significant decrease in surface biotinylated KCC2 (chronic stress = 17.74 ± 3.29, control = 43.41 ± 1.07 OD units/20 μg protein; n = 5 per experimental group) and S940 phosphorylated KCC2 in the hippocampus following chronic stress compared to control (chronic stress = 14.70.± 2.37, control = 29.23 ± 5.10 OD units/20 μg protein; n = 5 per experimental group) (p = .032 using a Student's unpaired t-test) (Figure 1c). The loss of KCC2 surface expression following chronic stress would be predicted to disrupt chloride homeostasis which may contribute to a stress induced increase in neuronal excitability.

A depolarizing shift in the $GABA_A$ reversal potential (E_{GABA}) is observed in CA1 pyramidal neurons following chronic stress

Lee et al (2011) have demonstrated a depolarizing shift in E_{GABA} in cultured neurons after dephosphorylation of KCC2 residue S940. Therefore, it was anticipated that a depolarizing shift in E_{GABA} would be observed following chronic (where KCC2 was downregulated) but not acute restraint stress when compared to unstressed controls. To investigate whether the dephosphorylation of KCC2 residue S940 following acute or chronic stress causes a shift in E_{GABA} in hippocampal principal neurons, gramicidin perforated patch recordings were performed on CA1 pyramidal neurons to prevent disruption of the native chloride gradients. The $GABA_A$ mediated current at each potential was determined by subtracting the current-voltage relationships in the presence and absence of the $GABA_A$R antagonist SR95331 ((Song et al., 2011) (Figure 2a and 2b). Compared to unstressed controls (−68.33 ± 2.31 mV; n = 9 cells/6 mice) no difference in E_{GABA} was observed following acute stress (−67.88 ± 2.11 mV; n = 9 cells/6 mice) in CA1 pyramidal neurons consistent with no observable change in hippocampal KCC2 expression following acute stress. However, a significant depolarizing shift in E_{GABA} was observed in CA1 pyramidal neurons following chronic stress (−60.26 ± 1.83 mV; n = 15 cells/11 mice) when compared to unstressed controls (p = .010 one-way ANOVA $F(2,30) = 5.379$ with a Tukey's post hoc test) (Figure 2c and 2e). Interesting although no difference in resting membrane potential (RMP) was

observed between control (−67.79 ± 1.74 mV; n = 13 cells/9 mice) and chronically stressed neurons (−66.79 ± 1.97 mV n = 17 cells/12 mice) a significant hyperpolarization of the membrane was observed following acute stress (−75.81 ± 1.57 mV n = 9 cells/6 mice) (p = .008 one-way ANOVA $F(2,36) = 5.494$ with a Tukey's post hoc test) (Figure 2d). Therefore whilst only 33% of control neurons exhibited depolarizing E_{GABA} values compared to their RMP, 80% of chronically stressed and 88% of acutely stressed neurons exhibited depolarizing E_{GABA} values (χ^2 (2, N = 33) = 7.958, p = .019) compared to hyperpolarizing/shunting responses. The fact that acutely stressed neurons presented with E_{GABA} values more depolarized than their resting membrane potential must be due entirely to the hyperpolarization of these neurons, because E_{GABA} remains unchanged compared to controls. Thus, opening of $GABA_AR$ in acutely stressed neurons will not move the membrane potential any closer to threshold. Rather the hyperpolarization of the membrane likely reduces neuronal excitability and contributes to the anti-convulsant effects of an acute stressor (Joels and Baram, 2009; Reddy and Rogawski, 2002). In contrast, E_{GABA} was shifted to a more depolarized potential following chronic stress thus $GABA_AR$ opening would be expected to move the membrane potential closer to AP threshold. Although this approximately 8 mV depolarizing shift in E_{GABA} is unlikely to be sufficient for an individual $GABA_A$-mediated postsynaptic potential to reach action potential threshold (and thus lead to the direct excitatory actions of GABA), GABA mediated membrane depolarizations may indirectly increase neuronal excitability by activating voltage dependent conductances such as the persistent sodium current (Cherubini et al., 2011; Valeeva et al., 2010) or by reducing the current required to reach AP threshold for coincident EPSCs thus increasing neuronal excitability. Indeed, direct inhibition of KCC2 with furosemide increases the excitability of neuron networks in culture (Deeb et al., 2013; Jarolimek et al., 1996) and in CA1 neurons in hippocampal slices (Thompson and Gahwiler, 1989).

The intrinsic excitability of CA1 pyramidal neurons are increased following chronic stress when the native chloride gradients are maintained

The intrinsic excitability of CA1 pyramidal neurons following chronic stress was examined using gramicidin perforated patch recordings. Input-output curves were generated by square wave current injections in 20 pA increments from 20 pA to 300 pA (Figure 3a) and as anticipated, a leftward shift in the input-output curves was observed following chronic restraint stress (Figure 3b). For example for a 60 pA current injection, CA1 pyramidal neurons from mice subjected to chronic stress fired at 10.95 ± 2.06 Hz (n = 21 cells/9 mice) compared to neurons from unstressed animals which fired at 3.89 ± 1.26 Hz (n = 19 cells/10 mice) (p = .002 using a one–way ANOVA ($F(2,54) = 6.717$) with a Dunnett's post hoc test) (Figure 3b and 3f). Consistent with this observation, the current required to reach action potential threshold (iAP) was significantly reduced for chronically stressed neurons (iAp = 32.93 ± 9.00 pA) when compared to unstressed controls (iAp = 58.68 ± 7.73 pA) (p = .028 using one-way ANOVA (F (2,54) = 3.833) with a Dunnett's post hoc test (Figure 3c and 3d). In addition to the effects on the iAP, we also observed a significant increase in the slope of the input-output curve in chronically stressed neurons (46.92 ± 2.58 Hz/pA) when compared to unstressed controls (38.68 ± 2.26 Hz/pA) (p < .001 using one-way ANOVA (F (2,54) = 9.31) with a Dunnett's post hoc test) (Figure 3f). This will further enhance neuronal excitability by increasing the sensitivity of the neuron to subtle increases in excitatory input.

Interestingly, despite the clear leftward shift in the input-output curves, chronically stressed neurons were significantly more excitable only at current injections less than 120 pA (Figure 3c). Indeed, no significant difference in the I_{50} (control = 143.73 ± 7.36 pA, chronic stress 129.81 ± 7.99 pA) or the firing frequency at the highest current injection (control = 40.98 ± 2.82 Hz, chronic stress = 46.51 ± 2.51 Hz, Figure 3c) were observed following chronic stress compared to unstressed controls.

To determine whether the increase in intrinsic excitability of CA1 pyramidal neurons following chronic stress is related to the depolarizing shift in E_{GABA}, we generated input-output curves in the presence of the NKCC1 inhibitor bumetanide, which has been shown to block depolarizing shifts in E_{GABA} (Barmashenko et al., 2011; Cleary et al., 2013; Dzhala et al., 2008; Huberfeld et al., 2007; Kim et al., 2011; Kim et al., 2013; Rheims et al., 2008; Sun et al., 2012; Tyzio et al., 2014; Witte et al., 2014) and compared the intrinsic excitability to that of unstressed control neurons (Figure 3c, 3e and 3f). The addition of 10 μM bumetanide to the bath prevented a leftward shift in the input output curve following chronic stress with no significant difference in the current required to reach AP threshold (iAP = 60.16 ± 6.37 pA; n = 17 cells/7 mice) compared to unstressed controls. No significant difference was also observed in the slope of the input-output relationship (33.71 ± 1.23 Hz/pA), the I_{50} (134.71 ± 7.24 pA) and the firing frequency at the highest current injection (46.00 ± 1.73 Hz) when compared to unstressed control neurons. The ability of bumetanide to rescue the chronic stress induced increase in intrinsic excitability suggests involvement of an intracellular chloride-dependent mechanism.

If disrupted chloride homeostasis plays a role in the stress-induced increase in CA1 pyramidal neuron excitability, it would be predicted that under conditions where the intracellular chloride concentration of control and stressed neurons are identical, as is the case in the whole cell configuration, that there would be no significant difference in neuronal excitability. As predicted, no significant difference was observed in the iAP between control and chronically stressed CA1 pyramidal neurons recorded in the whole-cell configuration (control iAp = 75.93 ± 10.97 pA; n = 17 cells/9 mice and chronic stress iAp = 76.09 ± 10.09 pA; n = 18 cells/9 mice) (Figure 4a–d). In addition no significant difference in slope (control = 33.24 ± 2.74 Hz/pA, chronic stress = 33.84 ± 2.11 Hz/pA) (Figure 4d), I_{50} (control = 145.21 ± 11.95 pA, chronic stress = 144.60 ± 8.71 pA) or maximum firing frequency (control = 39.41 ± 2.63 Hz, chronic stress = 38.50 ± 2.66 Hz) were found in the whole cell configuration (Figure 4b, 4d).

To investigate potential mechanisms underlying the increased intrinsic excitability of CA1 pyramidal neurons following chronic stress, phase plane analysis of whole cell recordings were performed on the first action potential generated in response to a 160 pA current injection. However, we did not observe a significant difference in the rate of AP rise or decay, AP peak, threshold or the after-hyperpolarization (AHP) (Figure 4e, Table 1; n = 15–18 cells per experimental group for control and chronic stress respectively).

No change in phasic inhibition in CA1 pyramidal neurons after chronic stress

Chronic stress has previously been shown to alter hippocampal GABAergic inhibition (Hu et al., 2010; Serra et al., 2006; Serra et al., 2008). To investigate possible changes in

GABAergic neurotransmission, spontaneous inhibitory postsynaptic currents (IPSCs) were recorded in the whole cell configuration in CA1 pyramidal neurons from control and chronically stressed mice. No significant difference was observed in IPSC frequency, peak, or τ (decay) between control (frequency: 14.94±0.75 Hz; peak: −35.09±3.09 pA;τ: 4.21±0.35 ms; n = 13 cells/7 mice) and slices from chronically stressed mice (frequency: 16.17±1.38 Hz; peak: −30.94±3.27 pA;τ: 4.50±0.33 ms; n = 13 cells/9 mice) (Table 2, Figure 5). Furthermore, there was no significant difference in the input conductance (control: 0.75 ± 0.08 nS/pF; n = 46 cells/12 mice, chronic stress: 0.86 ± 0.10 nS/pF; 45 cells/9 mice). These data suggest that neither a change in IPSC frequency or in the composition of postsynaptic $GABA_A$Rs in CA1 pyramidal neurons contribute to the shift in E_{GABA} observed following chronic stress.

Tonic inhibition is significantly increased in CA1 pyramidal neurons following chronic stress

The expression of the α_4 and δ $GABA_A$R subunits, which contribute to tonic inhibition, have been shown to increase in the hippocampus following chronic social isolation stress (Serra et al., 2006). These changes in subunit expression corresponded to an increase in tonic inhibition in the dentate gyrus and a greater sensitivity to the GABA mimetic THIP and the neurosteroid allopregnanolone (Holm et al., 2011; Serra et al., 2006). Greater tonic inhibition following chronic stress would be expected to increase the chloride load and contribute to the depolarizing shift in E_{GABA}. As predicted, the magnitude of tonic inhibition measured by the difference in baseline holding current in the presence and absence of GABAzine (SR95531) was significantly different between control (7.26 ± 1.96 pS/pF; n = 18 cells) and chronically stressed (20.68 ± 6.33 pS/pF; n = 12 cells) CA1 pyramidal neurons (Figure 6) (p = .025, Student's unpaired t-test). These data suggest that alterations in tonic inhibition contribute to the observed shift in E_{GABA} following chronic stress.

Chronic but not acute stress increases seizure severity which can be rescued by the NKCC1 inhibitor bumetanide

Chronic stress causes an increase in serum corticosterone, the dephosphorylation and downregulation of hippocampal KCC2 expression, a depolarizing shift in E_{GABA} and increased intrinsic excitability of CA1 pyramidal neurons. Based on these observations and the published literature (Chadda and Devaud, 2004; Jones et al., 2013; Matsumoto et al., 2003) we predicted that chronic stress would increases the severity of seizures induced with the chemical convulsant kainic acid (10 mg/kg by intraperitoneal (i.p.) injection). Furthermore, as the increased intrinsic excitability of CA1 pyramidal neurons following chronic stress could be rescued by blocking NKCC1 mediated chloride influx with bumetanide (Figure 4), we predicted that seizure severity following kainic acid administration (10mg/kg, i.p.) would be reduced when chronically stressed mice were treated with bumetanide (0.2mg/kg i.p.). The average duration of epileptiform activity per episode increased significantly following chronic stress (1194.70 ± 153.68 s) compared to control (443.82 ± 98.77 s) which could be rescued by a single dose of bumetanide (288.59 ± 79.51 s) (p < .001 using one-way ANOVA; F (2,29) = 15.74 and a Tukey's post hoc test). Similarly, chronically stressed mice spent a significantly greater percent time exhibiting

epileptiform activity (74.20 ± 2.13 %; n = 11) compared to control (54.20 ± 5.16 %; n =13) and chronically stressed mice administered bumetanide (40.29 ± 10.13 %) (p = .002 using one-way ANOVA; F(2,29) = 7.775 and a Tukey's post hoc test) (Figure 7). In contrast to chronic stress, no changes in KCC2 expression or E_{GABA} were observed following an acute restraint stress and thus, consistent with the published literature (for review see (Joels, 2009)), no increase in seizure severity was predicted following an acute stressor. Acute restraint stress significantly reduced the average duration of epileptiform activity per episode (144.08 ± 41.05 s) compared to minimally-handled controls (443.82 ± 98.77 s) (p = .012 using a unpaired Student's T-test), Furthermore, the percent time exhibiting epileptiform activity (29.13 ±7.75 %; n = 12) was reduced following acute stress compared to minimally-handled controls (54.20 ± 5.16 %; n =13) (p = .012 using a Student's unpaired t-test).

Discussion

Consistent with a reduction in hippocampal KCC2 surface expression following chronic stress (Figure 1), gramicidin perforated patch recording identified a depolarizing E_{GABA} shift in CA1 pyramidal neurons following chronic but not acute stress and an increase in the intrinsic neuronal excitability (Figure 3) The mechanism(s) whereby a shift in E_{GABA} could alter intrinsic neuronal excitability are currently unclear. Previous studies have demonstrated shifts in E_{GABA} associated with increased intrinsic excitability under pathological conditions, in which no change in resting membrane potential or input conductance was observed (Barmashenko et al., 2011), similar to our findings following chronic stress. Our data does, however, indicate that the increase in intrinsic neuronal excitability following chronic stress involves an intracellular chloride-dependent mechanism since it is blocked with bumetanide. Furthermore, any deficiencies in chloride extrusion due to a loss of KCC2 are likely to be exacerbated by the greater chloride load imparted by the increase in tonic inhibition (Figure 6). Further investigation into the mechanisms through which a depolarizing shift in E_{GABA} could alter intrinsic neuronal excitability are therefore necessary (for review see (Beck and Yaari, 2008). However, an anticipated outcome from a depolarizing shift in E_{GABA} is a reduction in the inhibitory driving force for GABA. Furthermore depolarizing $GABA_A$ receptor mediated currents will shift the membrane potential closer to threshold which may be sufficient to indirectly trigger action potential firing (Cherubini et al., 2011; Valeeva et al., 2010).

Animals with a partial knockdown of KCC2 experience hippocampal hyperexcitability, seizures and death (Woo et al., 2002). A reduction in total KCC2 protein has been demonstrated in animal models of epilepsy and has been implicated in epileptogenesis (Barmashenko et al., 2011; Bragin et al., 2009; Li et al., 2008; Pathak et al., 2007). Therefore, alterations in the expression of KCC2 may contribute to the precipitation of seizures associated with chronic stress with prolonged exposure to elevated serum corticosterone having been shown to accelerate epileptogenesis in rodent models (Jones et al., 2013; Karst et al., 1999; Kumar et al., 2007; Taher et al., 2005). The mechanism through which chronic stress triggers the dephosphorylation of S940 and downregulation of hippocampal KCC2 (Figure 1c) is currently unclear. This is particularly interesting considering that an acute stressor can trigger a robust downregulation of KCC2 in the hypothalamus (Hewitt et al., 2009; Inoue and Bains, 2014; Sarkar et al., 2011) but not in the

hippocampus (Figure 1) suggesting regional differences in the sensitivity to stress hormones. Elevated extracellular glutamate and NMDA receptor activation has been shown to induce dephosphorylation of S940, downregulation of KCC2 and a depolarizing shift in E_{GABA} (Deeb et al., 2013; Lee et al., 2011) via increased intracellular calcium and activation of PP1 may be involved (Lee et al., 2011). As extracellular glutamate and NMDA receptor expression have also been reported to be elevated in the hippocampus following chronic corticosterone treatment (Calabrese et al., 2012; Skorzewska et al., 2007; Weiland et al., 1997) an NMDA-mediated downregulation of KCC2 is an attractive candidate mechanism although, changes in other intracellular signaling cascades cannot be ruled out. Further research is required to identify the underlying mechanism(s) involved and identify potential candidates for therapeutic intervention.

The relationship between stress and epilepsy is dependent upon the nature and the duration of the stressor (for review see (Maguire and Salpekar, 2013). Unlike chronic stress, acute stress is protective against seizures ((De Lima and Rae, 1991; Pericic et al., 2000; Pericic et al., 2001; Reddy and Rogawski, 2002) (Figure 7) due in part to the elevation of stress derived neurosteroids which positively modulate GABAergic inhibition (Reddy and Rogawski, 2002). Although the underlying mechanism requires further investigation, we demonstrate that actutely stressed CA1 pyramidal cells exhibit a hyperpolarized RMP compared to control and chronically stressed neurons (Figure 2) which will likely reduce neuronal excitability and contribute to the protective effect of an acute stressor.

Whilst the long term goal is to develop KCC2 activators to restore GABAergic inhibition(Gagnon et al., 2013), inhibiting chloride influx through the sodium-potassium chloride cotransporter (NKCC1) has been shown to restore E_{Cl} (Barmashenko et al., 2011) and have antiepileptic properties in humans and rodents (Brandt et al., 2010; Eftekhari et al., 2013; Kahle et al., 2009; O'Toole et al., 2013) (for review see (Loscher et al., 2012)). Figures 3 and 7 demonstrate that blocking NKCC1 with bumetanide can restore neuronal excitability to unstressed levels and rescue the stressed induced increase in seizure susceptibility, further demonstrating the therapeutic potential of targeting cation-chloride co-transporters for seizure management.

Conclusions

This study demonstrated a dephosphorylation and downregulation of KCC2 in the hippocampus following chronic stress which was associated with a depolarizing shift in E_{GABA} and increased intrinsic excitability of CA1 pyramidal neurons. In addition chronically stressed mice exhibited a greater vulnerability to kainic acid induced seizures. Both the increase in intrinsic excitability of CA1 pyramidal neurons and the greater seizure susceptibility following chronic stress could be rescued with the NKCC1 inhibitor, bumetanide suggesting a role for disrupted chloride homeostasis in stress exacerbated seizures. To the best of our knowledge this is the first time that a loss of KCC2 function and a depolarizing shift in E_{GABA} has been observed in thehippocampus following chronic stress and may provide new therapeutic avenues for treatment of the epilepsies.

Acknowledgments

The authors are grateful to Dr. Steve Moss for the generous gift of the phospho-specific KCC2 residue S940 antibody. The authors would also like to thank Vallent Lee for editing the manuscript and Dr. Tarek Deeb for essential discussions throughout this study.

Grants

G. MacKenzie was supported by a postdoctoral fellowship from the American Epilepsy Society and Sunovion Pharmaceuticals, Inc. J. Maguire was supported by NIH Grant R01 NS073574 and a Research Grant from the Epilepsy Foundation.

Reference List

Barmashenko G, Hefft S, Aertsen A, Kirschstein T, Kohling R. Positive shifts of the GABAA receptor reversal potential due to altered chloride homeostasis is widespread after status epilepticus. Epilepsia. 2011; 52:1570–1578. [PubMed: 21899534]

Bean BP. The action potential in mammalian central neurons. Nat Rev Neurosci. 2007; 8:451–465. [PubMed: 17514198]

Beck H, Yaari Y. Plasticity of intrinsic neuronal properties in CNS disorders. Nat Rev Neurosci. 2008; 9:357–369. [PubMed: 18425090]

Ben-Ari Y. Excitatory actions of gaba during development: the nature of the nurture. Nat Rev Neurosci. 2002; 3:728–739. [PubMed: 12209121]

Ben-Ari Y, Khalilov I, Kahle KT, Cherubini E. The GABA excitatory/inhibitory shift in brain maturation and neurological disorders. Neuroscientist. 2012; 18:467–486. [PubMed: 22547529]

Bonislawski DP, Schwarzbach EP, Cohen AS. Brain injury impairs dentate gyrus inhibitory efficacy. Neurobiol Dis. 2007; 25:163–169. [PubMed: 17045484]

Boulenguez P, Liabeuf S, Bos R, Bras H, Jean-Xavier C, Brocard C, Stil A, Darbon P, Cattaert D, Delpire E, Marsala M, Vinay L. Down-regulation of the potassium-chloride cotransporter KCC2 contributes to spasticity after spinal cord injury. Nat Med. 2010; 16:302–307. [PubMed: 20190766]

Bragin DE, Sanderson JL, Peterson S, Connor JA, Muller WS. Development of epileptiform excitability in the deep entorhinal cortex after status epilepticus. Eur J Neurosci. 2009; 30:611–624. [PubMed: 19674083]

Brandt C, Nozadze M, Heuchert N, Rattka M, Loscher W. Disease-modifying effects of phenobarbital and the NKCC1 inhibitor bumetanide in the pilocarpine model of temporal lobe epilepsy. J Neurosci. 2010; 30:8602–8612. [PubMed: 20573906]

Calabrese F, Guidotti G, Molteni R, Racagni G, Mancini M, Riva MA. Stress-induced changes of hippocampal NMDA receptors: modulation by duloxetine treatment. PLoS One. 2012; 7:e37916. [PubMed: 22666412]

Castro OW, Santos VR, Pun RY, McKlveen JM, Batie M, Holland KD, Gardner M, Garcia-Cairasco N, Herman JP, Danzer SC. Impact of corticosterone treatment on spontaneous seizure frequency and epileptiform activity in mice with chronic epilepsy. PLoS One. 2012; 7:e46044. [PubMed: 23029379]

Chadda R, Devaud LL. Sex differences in effects of mild chronic stress on seizure risk and GABAA receptors in rats. Pharmacol Biochem Behav. 2004; 78:495–504. [PubMed: 15251258]

Cherubini E, Griguoli M, Safiulina V, Lagostena L. The depolarizing action of GABA controls early network activity in the developing hippocampus. Mol Neurobiol. 2011; 43:97–106. [PubMed: 21042953]

Cleary RT, Sun H, Huynh T, Manning SM, Li Y, Rotenberg A, Talos DM, Kahle KT, Jackson M, Rakhade SN, Berry G, Jensen FE. Bumetanide enhances phenobarbital efficacy in a rat model of hypoxic neonatal seizures. PLoS One. 2013; 8:e57148. [PubMed: 23536761]

Conrad CD. Chronic stress-induced hippocampal vulnerability: the glucocorticoid vulnerability hypothesis. Rev Neurosci. 2008; 19:395–411. [PubMed: 19317179]

de Groote L, Linthorst AC. Exposure to novelty and forced swimming evoke stressor-dependent changes in extracellular GABA in the rat hippocampus. Neuroscience. 2007; 148:794–805. [PubMed: 17693036]

De Lima TC, Rae GA. Effects of cold-restraint and swim stress on convulsions induced by pentylenetetrazol and electroshock: influence of naloxone pretreatment. Pharmacol Biochem Behav. 1991; 40:297–300. [PubMed: 1805234]

Deeb TZ, Nakamura Y, Frost GD, Davies PA, Moss SJ. Disrupted Cl(−) homeostasis contributes to reductions in the inhibitory efficacy of diazepam during hyperexcited states. Eur J Neurosci. 2013; 38:2453–2467. [PubMed: 23627375]

Drevets WC, Price JL, Furey ML. Brain structural and functional abnormalities in mood disorders: implications for neurocircuitry models of depression. Brain Struct Funct. 2008; 213:93–118. [PubMed: 18704495]

Dzhala VI, Brumback AC, Staley KJ. Bumetanide enhances phenobarbital efficacy in a neonatal seizure model. Ann Neurol. 2008; 63:222–235. [PubMed: 17918265]

Eftekhari S, Mehvari HJ, Najafi ZM, Hashemi Fesharaki SS, Gharakhani M, Mostafavi H, Joghataei MT, Beladimoghadam N, Rahimian E, Hadjighassem MR. Bumetanide reduces seizure frequency in patients with temporal lobe epilepsy. Epilepsia. 2013; 54:e9–12. [PubMed: 23061490]

Gagnon M, Bergeron MJ, Lavertu G, Castonguay A, Tripathy S, Bonin RP, Perez-Sanchez J, Boudreau D, Wang B, Dumas L, Valade I, Bachand K, Jacob-Wagner M, Tardif C, Kianicka I, Isenring P, Attardo G, Coull JA, De KY. Chloride extrusion enhancers as novel therapeutics for neurological diseases. Nat Med. 2013; 19:1524–1528. [PubMed: 24097188]

Gunn BG, Cunningham L, Cooper MA, Corteen NL, Seifi M, Swinny JD, Lambert JJ, Belelli D. Dysfunctional astrocytic and synaptic regulation of hypothalamic glutamatergic transmission in a mouse model of early-life adversity: relevance to neurosteroids and programming of the stress response. J Neurosci. 2013; 33:19534–19554. [PubMed: 24336719]

Haam J, Popescu IR, Morton LA, Halmos KC, Teruyama R, Ueta Y, Tasker JG. GABA is excitatory in adult vasopressinergic neuroendocrine cells. J Neurosci. 2012; 32:572–582. [PubMed: 22238092]

Hewitt SA, Wamsteeker JI, Kurz EU, Bains JS. Altered chloride homeostasis removes synaptic inhibitory constraint of the stress axis. Nat Neurosci. 2009; 12:438–443. [PubMed: 19252497]

Holm MM, Nieto-Gonzalez JL, Vardya I, Henningsen K, Jayatissa MN, Wiborg O, Jensen K. Hippocampal GABAergic dysfunction in a rat chronic mild stress model of depression. Hippocampus. 2011; 21:422–433. [PubMed: 20087886]

Hu W, Zhang M, Czeh B, Flugge G, Zhang W. Stress impairs GABAergic network function in the hippocampus by activating nongenomic glucocorticoid receptors and affecting the integrity of the parvalbumin-expressing neuronal network. Neuropsychopharmacol. 2010; 35:1693–1707.

Huberfeld G, Wittner L, Clemenceau S, Baulac M, Kaila K, Miles R, Rivera C. Perturbed chloride homeostasis and GABAergic signaling in human temporal lobe epilepsy. J Neurosci. 2007; 27:9866–9873. [PubMed: 17855601]

Inoue W, Bains JS. Beyond inhibition: GABA synapses tune the neuroendocrine stress axis. Bioessays. 2014; 36:561–569. [PubMed: 24648386]

Jarolimek W, Brunner H, Lewen A, Misgeld U. Role of chloride-homeostasis in the inhibitory control of neuronal network oscillators. J Neurophysiol. 1996; 75:2654–2657. [PubMed: 8793770]

Joels M. Stress, the hippocampus, and epilepsy. Epilepsia. 2009; 50:586–597. [PubMed: 19054412]

Joels M, Baram TZ. The neuro-symphony of stress. Nat Rev Neurosci. 2009; 10:459–466. [PubMed: 19339973]

Joels M, Karst H, Krugers HJ, Lucassen PJ. Chronic stress: implications for neuronal morphology, function and neurogenesis. Front Neuroendocrinol. 2007; 28:72–96. [PubMed: 17544065]

Jones NC, Lee HE, Yang M, Rees SM, Morris MJ, O'Brien TJ, Salzberg MR. Repeatedly stressed rats have enhanced vulnerability to amygdala kindling epileptogenesis. Psychoneuroendocrino. 2013; 38:263–270.

Kahle KT, Barnett SM, Sassower KC, Staley KJ. Decreased seizure activity in a human neonate treated with bumetanide, an inhibitor of the Na(+)-K(+)-2Cl(−) cotransporter NKCC1. J Child Neurol. 2009; 24:572–576. [PubMed: 19406757]

Kahle KT, Deeb TZ, Puskarjov M, Silayeva L, Liang B, Kaila K, Moss SJ. Modulation of neuronal activity by phosphorylation of the K-Cl cotransporter KCC2. Trends Neurosci. 2013; 36:726–737. [PubMed: 24139641]

Kahle KT, Rinehart J, Lifton RP. Phosphoregulation of the Na-K-2Cl and K-Cl cotransporters by the WNK kinases. Biochim Biophys Acta. 2010; 1802:1150–1158. [PubMed: 20637866]

Karst H, de Kloet ER, Joels M. Episodic corticosterone treatment accelerates kindling epileptogenesis and triggers long-term changes in hippocampal CA1 cells, in the fully kindled state. Eur J Neurosci. 1999; 11:889–898. [PubMed: 10103082]

Kim JS, Kim WB, Kim YB, Lee Y, Kim YS, Shen FY, Lee SW, Park D, Choi HJ, Hur J, Park JJ, Han HC, Colwell CS, Cho YW, Kim YI. Chronic hyperosmotic stress converts GABAergic inhibition into excitation in vasopressin and oxytocin neurons in the rat. J Neurosci. 2011; 31:13312–13322. [PubMed: 21917814]

Kim YB, Kim YS, Kim WB, Shen FY, Lee SW, Chung HJ, Kim JS, Han HC, Colwell CS, Kim YI. GABAergic excitation of vasopressin neurons: possible mechanism underlying sodium-dependent hypertension. Circ Res. 2013; 113:1296–1307. [PubMed: 24103391]

Kumar G, Couper A, O'Brien TJ, Salzberg MR, Jones NC, Rees SM, Morris MJ. The acceleration of amygdala kindling epileptogenesis by chronic low-dose corticosterone involves both mineralocorticoid and glucocorticoid receptors. Psychoneuroendocrino. 2007; 32:834–842.

Lai CW, Trimble MR. Stress and epilepsy. Journal of Epilepsy. 1997; 10:177–186.

Lee HH, Deeb TZ, Walker JA, Davies PA, Moss SJ. NMDA receptor activity downregulates KCC2 resulting in depolarizing GABA(A) receptor-mediated currents. Nat Neurosci. 2011; 14:736–743. [PubMed: 21532577]

Lee HH, Jurd R, Moss SJ. Tyrosine phosphorylation regulates the membrane trafficking of the potassium chloride co-transporter KCC2. Mol Cell Neurosci. 2010; 45:173–179. [PubMed: 20600929]

Lee HH, Walker JA, Williams JR, Goodier RJ, Payne JA, Moss SJ. Direct protein kinase C-dependent phosphorylation regulates the cell surface stability and activity of the potassium chloride cotransporter KCC2. J Biol Chem. 2007; 282:29777–29784. [PubMed: 17693402]

Lee V, Maguire J. Impact of inhibitory constraint of interneurons on neuronal excitability. J Neurophysiol. 2013; 110:2520–2535. [PubMed: 24027099]

Li X, Zhou J, Chen Z, Chen S, Zhu F, Zhou L. Long-term expressional changes of Na+-K+-Cl-co-transporter 1 (NKCC1) and K+-Cl-co-transporter 2 (KCC2) in CA1 region of hippocampus following lithium-pilocarpine induced status epilepticus (PISE). Brain Res. 2008; 1221:141–146. [PubMed: 18550034]

Loscher W, Puskarjov M, Kaila K. Cation-chloride cotransporters NKCC1 and KCC2 as potential targets for novel antiepileptic and antiepileptogenic treatments. Neuropharmacology. 2012; 69:62–74. [PubMed: 22705273]

Maguire J, Ferando I, Simonsen C, Mody I. Excitability changes related to GABAA receptor plasticity during pregnancy. J Neurosci. 2009; 29:9592–9601. [PubMed: 19641122]

Maguire J, Mody I. Neurosteroid synthesis-mediated regulation of GABA(A) receptors: relevance to the ovarian cycle and stress. J Neurosci. 2007; 27:2155–2162. [PubMed: 17329412]

Maguire J, Salpekar JA. Stress, seizures, and hypothalamic-pituitary-adrenal axis targets for the treatment of epilepsy. Epilepsy Behav. 2013; 26:352–362. [PubMed: 23200771]

Maguire JL, Stell BM, Rafizadeh M, Mody I. Ovarian cycle-linked changes in GABA(A) receptors mediating tonic inhibition alter seizure susceptibility and anxiety. Nat Neurosci. 2005; 8:797–804. [PubMed: 15895085]

Matsumoto K, Nomura H, Murakami Y, Taki K, Takahata H, Watanabe H. Long-term social isolation enhances picrotoxin seizure susceptibility in mice: up-regulatory role of endogenous brain allopregnanolone in GABAergic systems. Pharmacol Biochem Behav. 2003; 75:831–835. [PubMed: 12957225]

McEwen BS. Brain on stress: how the social environment gets under the skin. Proc Natl Acad Sci U S A. 2012; 109(Suppl 2):17180–17185. [PubMed: 23045648]

McEwen BS, Gianaros PJ. Stress- and allostasis-induced brain plasticity. Annu Rev Med. 2011; 62:431–445. [PubMed: 20707675]

Michelson HB, Wong RK. Excitatory synaptic responses mediated by GABAA receptors in the hippocampus. Science. 1991; 253:1420–1423. [PubMed: 1654594]

O'Toole KK, Hooper A, Wakefield S, Maguire J. Seizure-induced disinhibition of the HPA axis increases seizure susceptibility. Epilepsy Res. 2013; 108:29–43. [PubMed: 24225328]

Papp E, Rivera C, Kaila K, Freund TF. Relationship between neuronal vulnerability and potassium-chloride cotransporter 2 immunoreactivity in hippocampus following transient forebrain ischemia. Neuroscience. 2008; 154:677–689. [PubMed: 18472345]

Pathak HR, Weissinger F, Terunuma M, Carlson GC, Hsu FC, Moss SJ, Coulter DA. Disrupted dentate granule cell chloride regulation enhances synaptic excitability during development of temporal lobe epilepsy. J Neurosci. 2007; 27:14012–14022. [PubMed: 18094240]

Pavlides C, Nivon LG, McEwen BS. Effects of chronic stress on hippocampal long-term potentiation. Hippocampus. 2002; 12:245–257. [PubMed: 12000121]

Payne JA, Rivera C, Voipio J, Kaila K. Cation-chloride co-transporters in neuronal communication, development and trauma. Trends Neurosci. 2003; 26:199–206. [PubMed: 12689771]

Payne JA, Stevenson TJ, Donaldson LF. Molecular characterization of a putative K-Cl cotransporter in rat brain. A neuronal-specific isoform. J Biol Chem. 1996; 271:16245–16252. [PubMed: 8663311]

Pericic D, Jazvinscak M, Svob D, Mirkovic K. Swim stress alters the behavioural response of mice to GABA-related and some GABA-unrelated convulsants. Epilepsy Res. 2001; 43:145–152. [PubMed: 11164703]

Pericic D, Svob D, Jazvinscak M, Mirkovic K. Anticonvulsive effect of swim stress in mice. Pharmacol Biochem Behav. 2000; 66:879–886. [PubMed: 10973529]

Pittenger C, Duman RS. Stress, depression, and neuroplasticity: a convergence of mechanisms. Neuropsychopharmacol. 2008; 33:88–109.

Price TJ, Cervero F, Gold MS, Hammond DL, Prescott SA. Chloride regulation in the pain pathway. Brain Res Rev. 2009; 60:149–170. [PubMed: 19167425]

Reddy DS, Rogawski MA. Stress-induced deoxycorticosterone-derived neurosteroids modulate GABA(A) receptor function and seizure susceptibility. J Neurosci. 2002; 22:3795–3805. [PubMed: 11978855]

Rheims S, Minlebaev M, Ivanov A, Represa A, Khazipov R, Holmes GL, Ben-Ari Y, Zilberter Y. Excitatory GABA in rodent developing neocortex in vitro. J Neurophysiol. 2008; 100:609–619. [PubMed: 18497364]

Rinehart J, Vazquez N, Kahle KT, Hodson CA, Ring AM, Gulcicek EE, Louvi A, Bobadilla NA, Gamba G, Lifton RP. WNK2 kinase is a novel regulator of essential neuronal cation-chloride cotransporters. J Biol Chem. 2011; 286:30171–30180. [PubMed: 21733846]

Rivera C, Li H, Thomas-Crusells J, Lahtinen H, Viitanen T, Nanobashvili A, Kokaia Z, Airaksinen MS, Voipio J, Kaila K, Saarma M. BDNF-induced TrkB activation down-regulates the K+-Cl- cotransporter KCC2 and impairs neuronal Cl-extrusion. J Cell Biol. 2002; 159:747–752. [PubMed: 12473684]

Rivera C, Voipio J, Thomas-Crusells J, Li H, Emri Z, Sipila S, Payne JA, Minichiello L, Saarma M, Kaila K. Mechanism of activity-dependent downregulation of the neuron-specific K-Cl cotransporter KCC2. J Neurosci. 2004; 24:4683–4691. [PubMed: 15140939]

Sarkar J, Wakefield S, Mackenzie G, Moss SJ, Maguire J. Neurosteroidogenesis Is Required for the Physiological Response to Stress: Role of Neurosteroid-Sensitive GABAA Receptors. J Neurosci. 2011; 31:18198–18210. [PubMed: 22171026]

Serra M, Mostallino MC, Talani G, Pisu MG, Carta M, Mura ML, Floris I, Maciocco E, Sanna E, Biggio G. Social isolation-induced increase in alpha and delta subunit gene expression is associated with a greater efficacy of ethanol on steroidogenesis and GABA receptor function. J Neurochem. 2006; 98:122–133. [PubMed: 16805802]

Serra M, Pisu MG, Mostallino MC, Sanna E, Biggio G. Changes in neuroactive steroid content during social isolation stress modulate GABAA receptor plasticity and function. Brain Res Rev. 2008; 57:520–530. [PubMed: 17920688]

Skorzewska A, Bidzinski A, Hamed A, Lehner M, Turzynska D, Sobolewska A, Walkowiak J, Plaznik A. Changes in hippocampal amino acid concentrations after chronic administration of corticosterone. Pharmacol Rep. 2007; 59:763–772. [PubMed: 18195468]

Song I, Savtchenko L, Semyanov A. Tonic excitation or inhibition is set by GABA(A) conductance in hippocampal interneurons. Nat Commun. 2011; 2:376. [PubMed: 21730957]

Sun L, Yu Z, Wang W, Liu X. Both NKCC1 and anion exchangers contribute to Cl(−) accumulation in postnatal forebrain neuronal progenitors. Eur J Neurosci. 2012; 35:661–672. [PubMed: 22390178]

Taher TR, Salzberg M, Morris MJ, Rees S, O'Brien TJ. Chronic low-dose corticosterone supplementation enhances acquired epileptogenesis in the rat amygdala kindling model of TLE. Neuropsychopharmacol. 2005; 30:1610–1616.

Thompson SM, Gahwiler BH. Activity-dependent disinhibition. II. Effects of extracellular potassium, furosemide, and membrane potential on ECl- in hippocampal CA3 neurons. J Neurophysiol. 1989; 61:512–523. [PubMed: 2709097]

Tyzio R, Nardou R, Ferrari DC, Tsintsadze T, Shahrokhi A, Eftekhari S, Khalilov I, Tsintsadze V, Brouchoud C, Chazal G, Lemonnier E, Lozovaya N, Burnashev N, Ben-Ari Y. Oxytocin-mediated GABA inhibition during delivery attenuates autism pathogenesis in rodent offspring. Science. 2014; 343:675–679. [PubMed: 24503856]

Ulrich-Lai YM, Herman JP. Neural regulation of endocrine and autonomic stress responses. Nat Rev Neurosci. 2009; 10:397–409. [PubMed: 19469025]

Valeeva G, Abdullin A, Tyzio R, Skorinkin A, Nikolski E, Ben-Ari Y, Khazipov R. Temporal coding at the immature depolarizing GABAergic synapse. Front Cell Neurosci. 2010; 4:17. [PubMed: 20725525]

Weiland NG, Orchinik M, Tanapat P. Chronic corticosterone treatment induces parallel changes in N-methyl-D-aspartate receptor subunit messenger RNA levels and antagonist binding sites in the hippocampus. Neuroscience. 1997; 78:653–662. [PubMed: 9153648]

Witte M, Reinert T, Dietz B, Nerlich J, Rubsamen R, Milenkovic I. Depolarizing chloride gradient in developing cochlear nucleus neurons: Underlying mechanism and implication for calcium signaling. Neuroscience. 2014; 261:207–222. [PubMed: 24388924]

Woo NS, Lu J, England R, McClellan R, Dufour S, Mount DB, Deutch AY, Lovinger DM, Delpire E. Hyperexcitability and epilepsy associated with disruption of the mouse neuronal-specific K-Cl cotransporter gene. Hippocampus. 2002; 12:258–268. [PubMed: 12000122]

Yu J, Proddutur A, Elgammal FS, Ito T, Santhakumar V. Status epilepticus enhances tonic GABA currents and depolarizes GABA reversal potential in dentate fast-spiking basket cells. J Neurophysiol. 2013; 109:1746–1763. [PubMed: 23324316]

Zhu L, Polley N, Mathews GC, Delpire E. NKCC1 and KCC2 prevent hyperexcitability in the mouse hippocampus. Epilepsy Res. 2008; 79:201–212. [PubMed: 18394864]

Highlights

- Chronic stress dephosphorylates and downregulates surface expression of KCC2.
- Chronic stress shifts EGABA in CA1 pyramidal neurons.
- Chronic stress increases seizure susceptibility and excitability of neurons in CA1.
- Bumetanide reverses chronic stress-induced increased CA1 neuronal excitability.

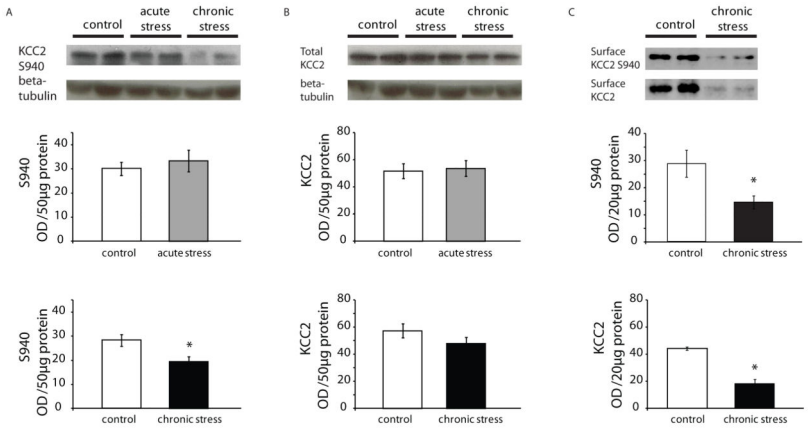

Figure 1. Phosphorylation of KCC2 residue S940 is reduced in the hippocampus after chronic but not acute restraint stress and corresponds to a loss of surface expression

A) No difference in S940 phosphorylated KCC2 was observed following an acute stress however a significant reduction was observed following chronic stress. B) No difference in total KCC2 was observed after acute stress (n = 12) or chronic stress (n = 13). Representative western blots from two independent samples for S940 and total KCC2 are shown with their corresponding β-tubulin controls below. C) The dephosphorylation of KCC2 S940 corresponded to a loss of surface expression of total and S940 phosphorylated KCC2. Representative western blots from two independent samples for surface S940 and total KCC2 are shown. Histograms represent the average optical density. Error bars represent ± SEM. * denotes significance ($P < 0.05$) compared to unstressed control using a Student's un-paired t-test.

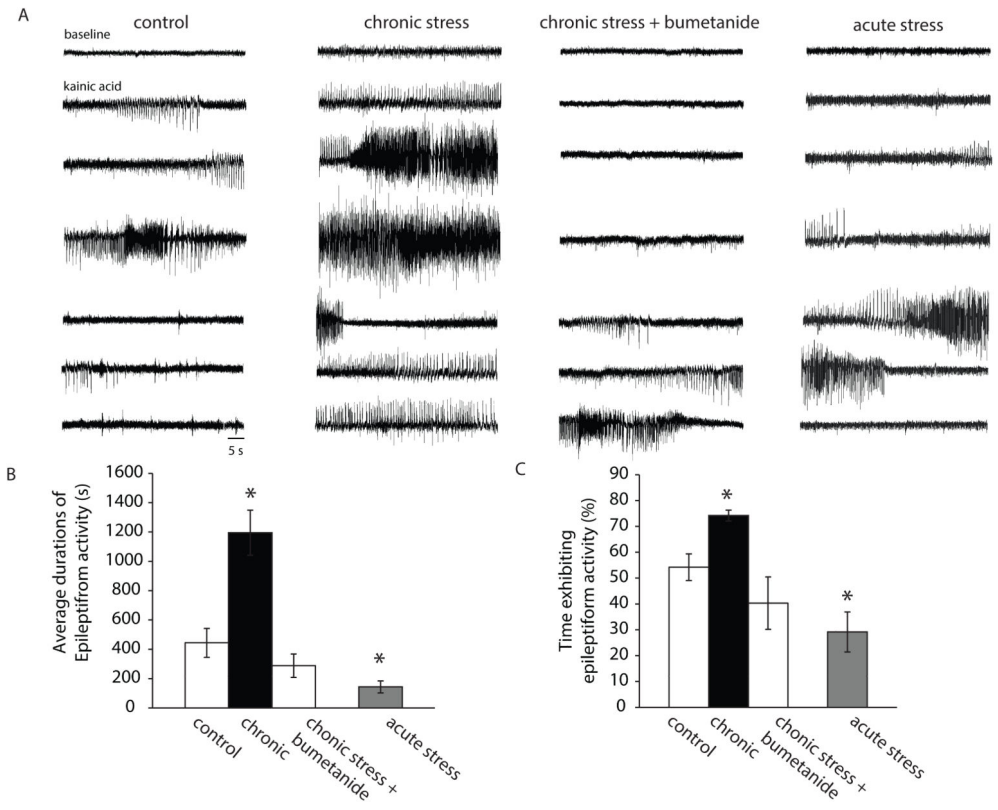

Figure 2. The $GABA_A$ reversal potential (E_{GABA}) is significantly m0ore depolarized in CA1 pyramidal neurons after chronic but not acute stress

A) Typical voltage clamp recording from a chronically stressed CA1 pyramidal neuron in response to 2 second square wave voltage steps ranging from −90 to −40 mV (in 5 mV increments) in the absence (black) and presence (grey) of GABAzine. B) Subtracting the current-voltage curves in the presence and absence of GABAzine revealed the $GABA_A$ mediated current. Data were fitted with a 2nd order polynomial function to calculate E_{GABA}. Arrow indicates the RMP. C) Chronic, but not acute stress results in a depolarizing shift in E_{GABA}. Individual data points for control, acute and chronic stress are shown (black lines) with the average in grey (n = 9 – 15 cells, 6 – 11 mice). D) Although there was no change in E_{GABA}, a significant hyperpolarization of the RMP was observed following acute stress. No significant change in RMP was observed following chronic stress. (n = 9 – 17 cells, 6 – 12 mice) E) The average current-voltage relationships for control (white), acute stress (grey) and chronic stress (black). Data were normalized to the current generated in response to a −90mV voltage step. Error bars indicate ± SEM, * = $P < 0.05$, one-way ANOVA with a Tukey's post-hoc test.

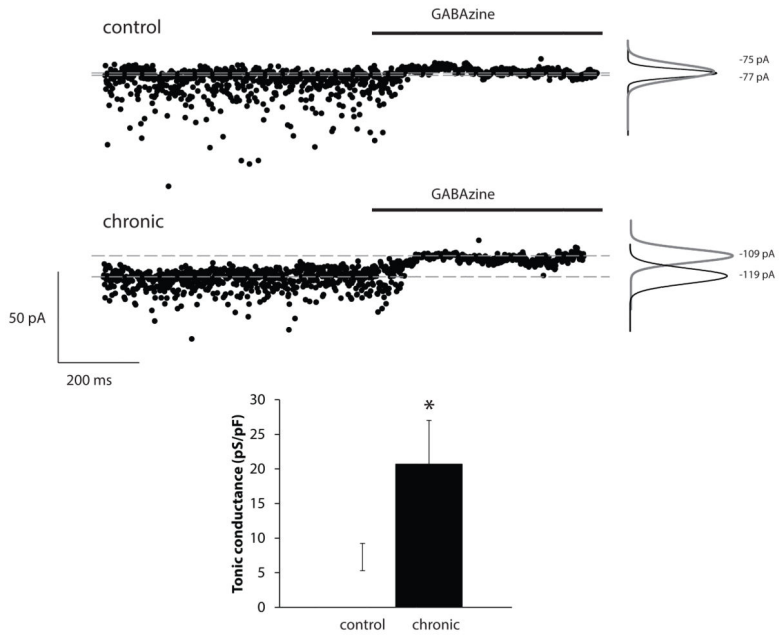

Figure 3. Chronic stress increases intrinsic CA1 pyramidal cell excitability when recorded in the perforated patch configuration

Input-output curves were generated in the perforated patch recording configuration so as not to disrupt the native chloride gradient. A) Typical current clamp recordings from control and chronically stressed CA1 pyramidal neurons. For clarity only the responses from the first 4 steps (20 – 80 pA in 20 pA increments) are shown. Resting membrane potential is also shown and recordings were performed without any additional applied current. B) Expanded averaged input-output curves for current injections from 20 – 120 pA for control (white circles; n = 19 cells, 10 mice) and chronic stress (black circles; n = 21 cells, 9 mice) CA1 pyramidal neurons. C) Complete input-output curves for control, chronic stress and chronic stress with bumetanide is shown as a Boltzmann function fitted to the averaged data. Chronic stress (dashed line) increased the excitability of CA1 pyramidal neurons compared to control (black line) at current injections less than 120 pA. This increased excitability was reduced by the addition of 10μM bumetanide to the extracellular solution (grey line). D) To calculate the average slope, I_{50} and maximum response individual input-output curves were fitted with a Boltzmann function (grey) of the form $f(W) = (MAX/(1 + \exp((I_{50}-I)/k)$, where I is current injected, MAX is the maximum response, k is a slope factor, and I_{50} is the current injection amplitude that elicits 50% of MAX. The current to AP threshold (iAP) was extrapolated from fitting a linear regression (black) to the initial rising phase. E) Chronic stress caused a significant reduction in the current required to reach action potential (iAP) which returned to control levels in the presence of bumetanide. F) Chronic stress causes a significant increase in the slope of the input-output relationship and a significant increase in firing frequency in response to a 60 pA current injection compared to control. * = $P < 0.05$. Errors bars = ± SEM.

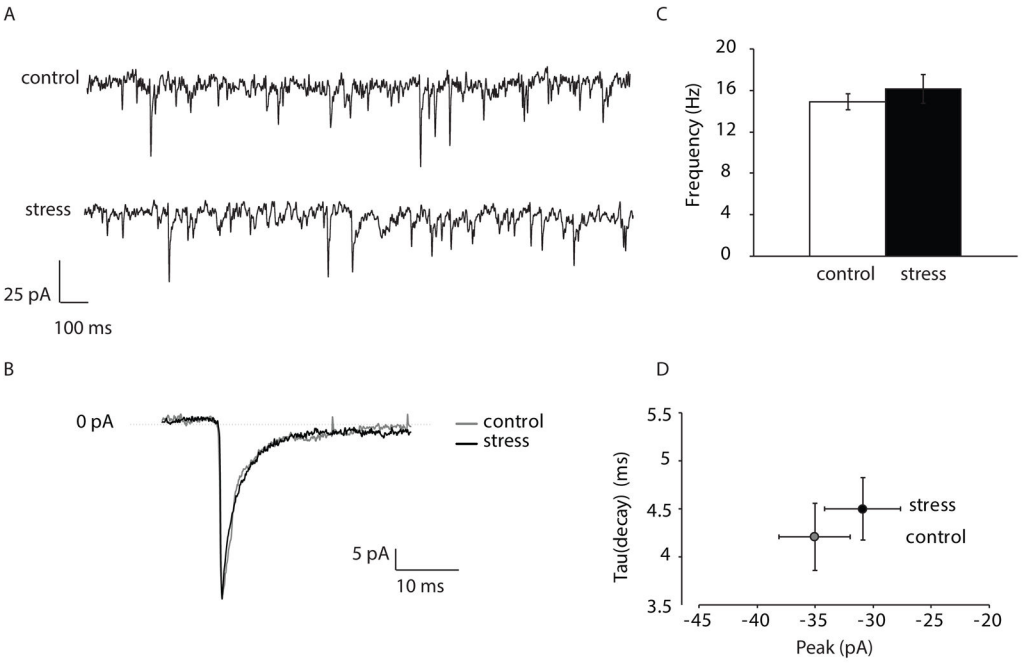

Figure 4. No difference in CA1 pyramidal cell excitability between the chronic stress and control groups when recordings are performed in the whole cell configuration

A) Typical current clamp recordings from control and stressed CA1 pyramidal neuron in response to current injections from 20–80 pA in 20 pA increments. The resting membrane potential is shown and apart from during the square wave current injections, recordings were performed without any additional applied current. Voltage protocol is shown below. B) Averaged input-output curves generated from control (white circle; n = 17 cells, 9 mice) and stress (black circle; n = 18 cells, 9 mice) CA1 pyramidal cell neurons in the whole cell configuration where the internal chloride concentration was clamped to 14 mM (see methods). C) Contrary to the perforated patch recordings, no significant difference in firing frequency between control or stressed CA1 pyramidal neurons was found in response to a 60 pA current injection. D) Averaged data highlighting the similarity between control (grey) and chronically stressed (black) neurons in the slope of the input-output relationship and the current to AP threshold. Additional phaseplane analysis was performed on the first action potential generated in response to a 160pA current injection. This analysis provides a fit independent estimate of the maximum rate of AP rise, decay, peak and threshold. E) Two typical action potentials generated (grey = control, black = chronic stress) in response to a 160 pA current injection are shown. Note the lack of difference in the max rate of rise, decay, AP peak or the AHP, (see also Table 1). Error bars = ± SEM.

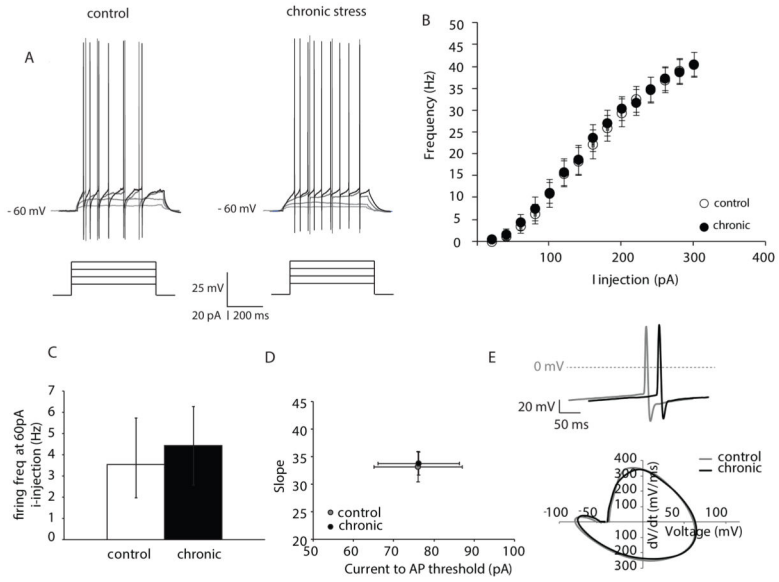

Figure 5. No difference in sIPSC properties in CA1 pyramidal neurons after chronic stress

A) Representative voltage clamp recordings at −60 mV from unstressed control and chronically stressed CA1 pyramidal cell neurons. B) Representative averaged waveforms from control (grey) and chronically stressed (black) neurons. Note the superimposition of the traces. No significant difference was observed in sIPSC frequency (C), the τ (decay) or the peak (D). Error bars = ± SEM, n = 13 cells, 7–9 mice.

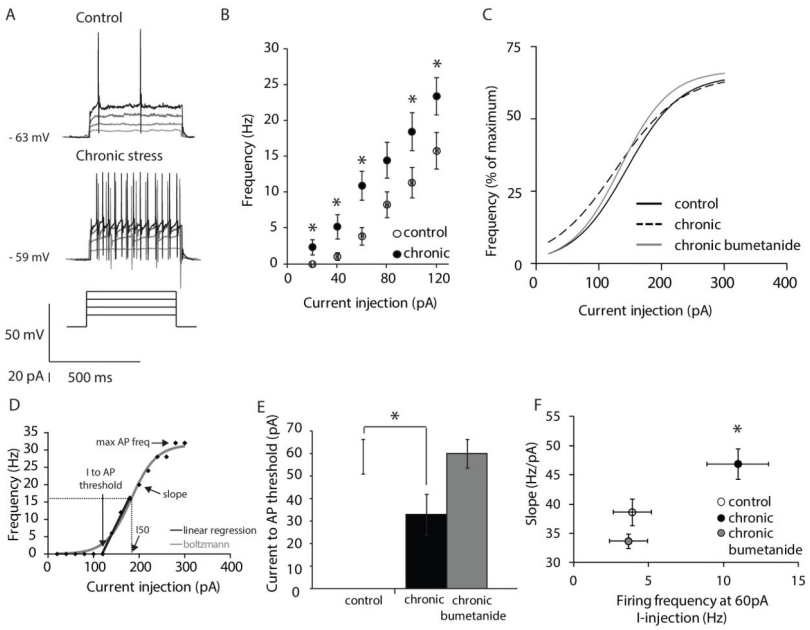

Figure 6. Tonic inhibition is increased following chronic stress

A) Representative traces showing the magnitude of tonic conductance in control (top) and chronically stressed (bottom) CA1 pyramidal neurons. Black bars represent the addition of GABAzine (SR95531). Tonic conductance was determined by the difference in current before and after the addition of GABAzine and normalized to capacitance. Mean current was determined by Gaussian fits to all point histograms for baseline currents (grey) and in the presence of GABAzine (black). B) Quantification of tonic current shows a significant increase in the tonic conductance following chronic stress. . * = $p < 0.05$. Error bars = ± SEM.

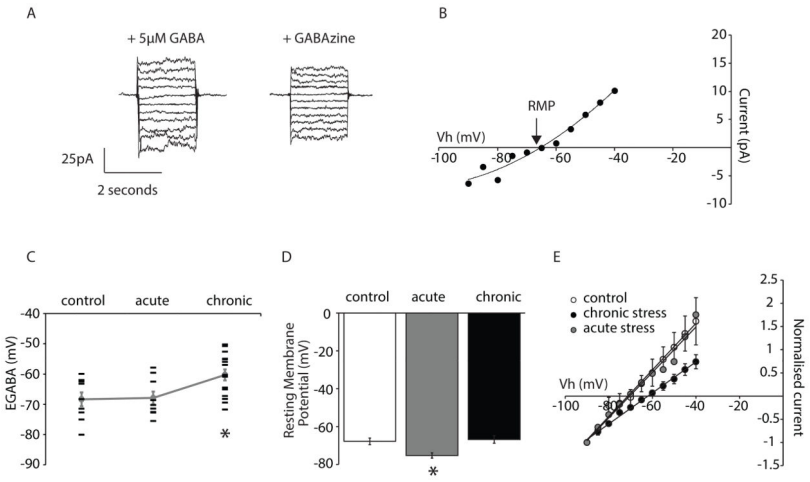

Figure 7. Chronic restraint stress is proconvulsant in a kainic acid seizure model

A. Representative *in vivo* EEG traces showing epileptiform activity 30 minutes following kainic acid injection. Each line represents 1 min of EEG activity for a total of 6 minutes for each experimental group. For the bumetanide condition, chronically stressed mice were administered bumetanide (0.2 mg/kg) following the final stressor and 30 minutes prior to kainic acid. B. The duration per episode of epileptiform activity was significantly increased following chronic restraint stress compared to, chronic stress with bumetanide and minimally-handled control animals. In contrast the duration per episode of epileptiform activity was significantly reduced following acute restraint stress compared to control. C. Mice subjected to chronic restraint stress spent a greater percent time exhibiting epileptiform activity compared to chronically stressed animals with bumetanide and unstressed controls. Again, mice subjected to an acute restraint stress spent significantly less percent time exhibiting epileptiform activity compared to unstressed controls. * = $p < 0.05$. Error bars = ± SEM.

Table 1

Action potential properties of control and chronically stressed CA1 pyramidal cell neurons

Action potential (AP) threshold, max rate of rise, max rate of decay, peak, and the peak of the after-hyperpolariztion potential (AHP) were all estimated from phase plane analysis on the first action potential generated in response to a 160pA current injection (see Figure 5). AHP height was calculated as the difference between the AHP peak and the AP threshold. Note that not all control neurons fired in response to a 160pA current injection. Control: n=15 cells, 9 mice. Chronic stress: n = 18 cells, 9 mice.

	control (±SEM)	chronic stress (±SEM)
AP threshold (mV)	−39.04 ±1.37	−38.96 ±1.28
max rate of rise (mV/m/s)	246.96 ±27.40	269.82 ±32.01
max rate of decay (mV/ms)	−179.39 ±16.41	−178.42 ±16.66
peak (mV)	53.16 ±3.92	53.53 ±4.11
AHP peak (mV)	−73.83 ±3.27	−70.28 ±2.29
AHP height (mV)	34.75 ±2.40	31.33 ±1.52

Table 2

sIPSC properties from control and chronically stressed CA1 pyramidal neurons

No significant difference in sIPSC properties were observed after chronic stress. Recordings were performed in the presence of 3mM kynurenic acid to block the glutamatergic component and 2mM QX-314 to inhibit AP firing.

	control (±SEM)	Chronic stress (±SEM)
Frequency (Hz)	14.94 ± 0.75	16.17 ± 1.38
Peak (pA)	−35.09 ± 3.09	−30.94 ± 3.27
τ(decay)	4.21 ± 0.35	4.50 ± 0.33